OPEN

Oncogene (2015), 1–13

www.nature.com/onc

ORIGINAL ARTICLE

MDM4/HIPK2/p53 cytoplasmic assembly uncovers coordinated repression of molecules with anti-apoptotic activity during early DNA damage response

F Mancini[1,2], L Pieroni[3,4], V Monteleone[1], R Lucà[1], L Fici[1,5], E Luca[1,2], A Urbani[3,4], S Xiong[6], S Soddu[7], R Masetti[5], G Lozano[6], A Pontecorvi[2] and F Moretti[1]

The p53 inhibitor, MDM4 (MDMX) is a cytoplasmic protein with p53-activating function under DNA damage conditions. Particularly, MDM4 promotes phosphorylation of p53 at Ser46, a modification that precedes different p53 activities. We investigated the mechanism by which MDM4 promotes this p53 modification and its consequences in untransformed mammary epithelial cells and tissues. In response to severe DNA damage, MDM4 stimulates p53Ser46^P by binding and stabilizing serine–threonine kinase HIPK2. Under these conditions, the p53-inhibitory complex, MDM4/MDM2, dissociates and this allows MDM4 to promote p53/HIPK2 functional interaction. Comparative proteomic analysis of DNA damage-treated cells versus -untreated cells evidenced a diffuse downregulation of proteins with anti-apoptotic activity, some of which were targets of p53Ser46^P/HIPK2 repressive activity. Importantly, MDM4 depletion abolishes the downregulation of these proteins indicating the requirement of MDM4 to promote p53-mediated transcriptional repression. Consistently, MDM4-mediated HIPK2/p53 activation precedes HIPK2/p53 nuclear translocation and activity. Noteworthy, repression of these proteins was evident also in mammary glands of mice subjected to γ-irradiation and was significantly enhanced in transgenic mice overexpressing MDM4. This study evidences the flexibility of MDM2/MDM4 heterodimer, which allows the development of a positive activity of cytoplasmic MDM4 towards p53-mediated transcriptional function. Noteworthy, this activity uncovers coordinated repression of molecules with shared anti-apoptotic function which precedes active cell apoptosis and that are frequently overexpressed and/or markers of tumour phenotype in human cancer.

Oncogene advance online publication, 11 May 2015; doi:10.1038/onc.2015.76

INTRODUCTION

MDM4 (also MDMX) is a master regulator of p53. It binds its homologue MDM2, and the resulting heterodimer represses p53 activity and controls p53 protein levels through MDM2-driven ubiquitination.[1,2] In addition, MDM4 negatively controls p53 transcriptional activity.[3] Conversely under DNA damage, MDM4 that is mostly a cytoplasmic protein,[4] is able to cooperate with p53 by enhancing stress-induced p53 stabilization[5–8] and promoting p53 mitochondrial apoptotic activity.[9–11] The presence of MDM4 has been associated to some post-translational modifications of p53.[9,11,12] Particularly, knockdown of MDM4 decreases phosphorylation of p53 at Ser46, a modification that has been linked to different p53 activities. P53Ser46^P is necessary for the transcriptional activation of the proapoptotic target AIP1[13] and is considered a mark of p53 apoptotic function.[14,15] Furthermore, this phosphorylation precedes and promotes p53 acetylation that in turn is involved in the transcriptional activation of some apoptotic targets.[16] P53Ser46^P is also relevant in the transcriptional repressive activity of p53.[17,18] More recently, it has been involved in the cytoplasmic apoptotic function of p53, p53Ser46^P being the functional form of p53 at the mitochondria.[9,11,19] The functional consequences of MDM4-mediated regulation of p53Ser46^P remain unknown.

Recently, two studies reported that mice-expressing MDM4 mutants defective in MDM2 binding, die during embryonic development despite the association of MDM4 to p53.[20,21] These data reinforce the hypothesis that the association between MDM4 and p53 may have different outcomes depending on additional factors such as its heterodimerization to MDM2. Therefore, the comprehension of MDM4 activity towards p53 is relevant also to understand the inhibitory activity of MDM4/MDM2 heterodimer towards p53.

In this work, we have investigated the mechanism by which MDM4 affects p53Ser46^P, as well as the functional consequences in mammary epithelial cells and tissues.

RESULTS

MDM4 binds and stabilizes HIPK2

Previous studies indicate an association between the levels of MDM4 and p53Ser46^P.[9,11] To understand whether this increase is attributable to a direct activity of MDM4, we analysed the effects of MDM4 towards serine–threonine kinases responsible for such phosphorylation. We focused on HIPK2, a homeodomain-interacting protein kinase, functioning as coregulator of p53[22,23]

[1]Institute of Cell Biology and Neurobiology, National Research Council of Italy (CNR), Roma, Italy; [2]Department of Endocrinology and Metabolism, Catholic University of Roma, Roma, Italy; [3]Proteomic and Metabolomic Laboratory, Fondazione Santa Lucia, Roma, Italy; [4]Department of Experimental Medicine and Surgery, University of Roma 'Tor Vergata', Roma, Italy; [5]Department of Obstetrics and Gynaecology, Catholic University of Roma, Roma, Italy; [6]Department of Genetics, M.D. Anderson Cancer Center, Houston, TX, USA and [7]Regina Elena National Cancer Institute, Roma, Italy. Correspondence: Dr F Moretti or Dr F Mancini, Institute of Cell Biology and Neurobiology, National Research Council of Italy (CNR), Via del Fosso di Fiorano, 64, Roma 00143, Italy.
E-mail: fabiola.moretti@cnr.it or francesca.mancini@ibcn.cnr.it
Received 2 July 2014; revised 2 February 2015; accepted 18 February 2015

and interacting with the MDM4 homologue, MDM2.[24] Given the frequent mutational or epigenetic inactivation of DNA damage pathways in cancer cell lines, we used immortalized MCF10A and primary HMEC breast cell lines. MCF10A cells were transfected with stealth MDM4-specific (si*MDM4*-MCF10A) or stealth control RNA (si*CTL*-MCF10A), and at 48 h after transfection exposed to adriamycin (Adr), known to induce double-strand breaks and to activate p53.[25] Exposure to 2 μM Adr caused a progressive cell death concomitant with decrease of the cell cycle inhibitor $p21^{WAF1}$ (Figure 1a, Supplementary Figure 1a).[26,27] Knockdown of MDM4 decreased $p53Ser46^{P}$ levels concurrent with a decrease of caspase-3 cleavage and PARP-p85 cleaved forms, indicating a reduction of the apoptotic process (Figure 1a, Supplementary Figure 1b). Interestingly, this coincides with a strong reduction of

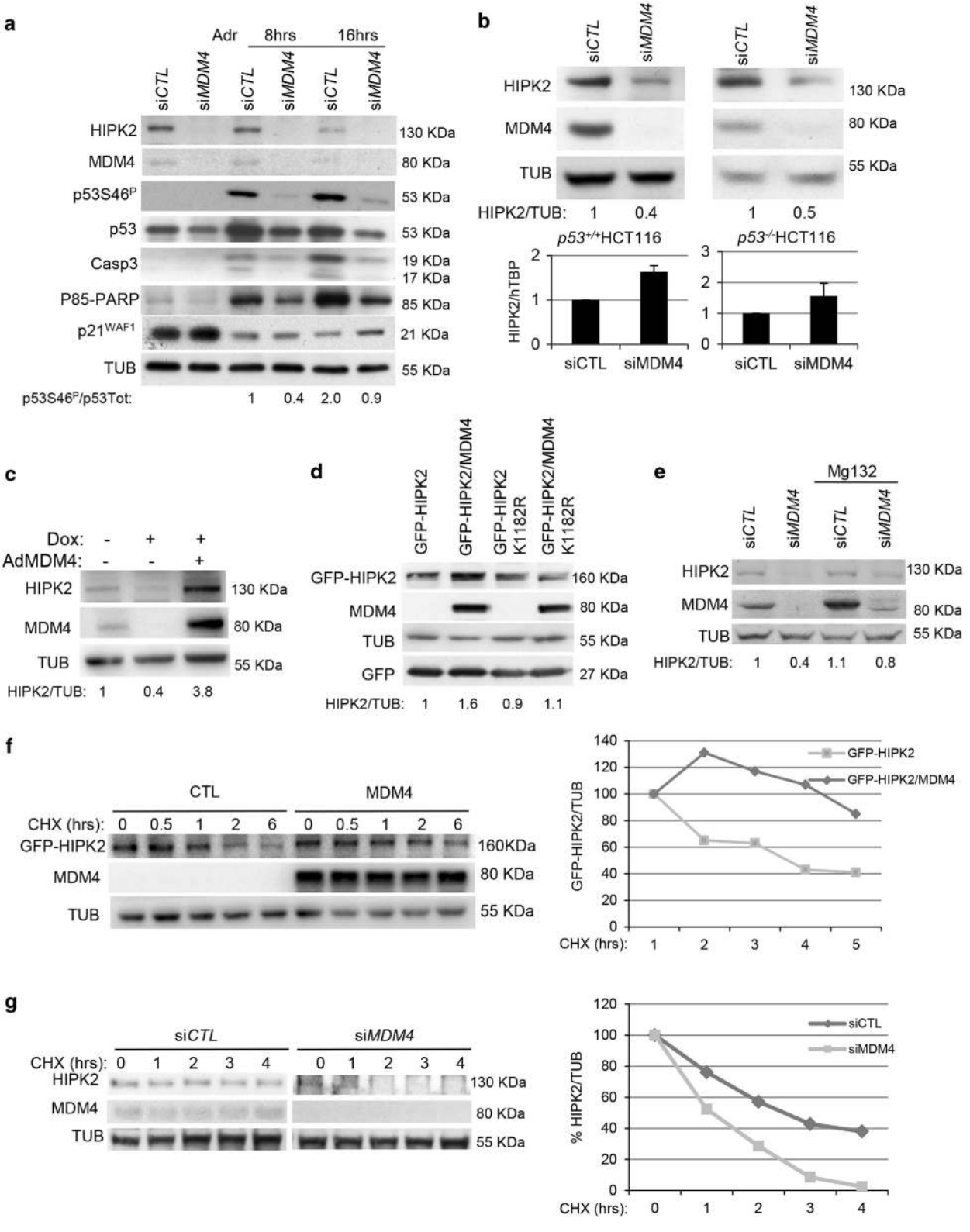

HIPK2 protein levels. In the absence of Adr, siMDM4 reduced cell proliferation and increased $p21^{WAF1}$ levels, in agreement with its inhibitory activity towards p53 (Figure 1a, Supplementary Figure 1c).[12,28] Analysis of HMEC exposed to Adr confirmed these data (Supplementary Figures 1d and e).

On the opposite, MDM4 overexpression increased the levels of GFP-HIPK2 and of $p53Ser46^P$ (Supplementary Figure 1f), although less efficiently than upon MDM4 depletion, supporting the hypothesis of a relationship between MDM4 and HIPK2. Reduction of HIPK2 by si*MDM4* occurred independently of p53 and did not correlate with reduction of *HIPK2* mRNA (Figure 1b, Supplementary Figure 1g), indicating that it occurs at the protein levels. Re-expression of adeno-MDM4 rescued the decrease of HIPK2 levels caused by doxycycline-inducible interference of MDM4 in MCF10A (Tet-sh-MDM4; Figure 1c), confirming the specificity of MDM4 activity. A GFP-HIPK2 mutant that cannot be degraded, HIPK2-K1182R[24] was insensitive to the expression of MDM4 (Figure 1d) and proteasome inhibitor MG132 partly rescued HIPK2 downregulation caused by si*MDM4* (Figure 1e), indicating that MDM4 counteracts HIPK2 degradation. Analysis of protein stability indeed revealed an increased half-life of GFP-HIPK2 when coexpressed with MDM4 (Figure 1f) and a decreased half-life of endogenous HIPK2 upon depletion of MDM4 (Figure 1g).

To determine whether MDM4 directly controls HIPK2 stability, the association between the two proteins was tested. MDM4 co-immunoprecipitated HIPK2, both when the two proteins were overexpressed (Figure 2a) as well as when endogenous (Figures 2b and c), indicating that the two proteins interact. The association was further increased by adryamicin, whereas it was reduced by *siMDM4* confirming the specificity of the interaction (Figure 2c). To assess whether MDM4 stabilizes HIPK2 depending on their association, the region/s of MDM4 involved in this interaction were identified. Two MDM4 deletion mutants, MDM4ΔBD and MDM4ΔRING (Figure 2d), coexpressed with GFP-HIPK2 in $Mdm4^{-/-}p53^{-/-}$ mouse embryonic fibroblasts (MEFs), were able to bind GFP-HIPK2 with efficiency similar to wt-MDM4, indicating that the central domain of MDM4 (aa106–360), common to both mutants, is involved in the interaction (Figure 2e). HIPK2 levels were increased by these mutants as much as by wt-MDM4, suggesting that the interaction modulates MDM4 stabilizing activity (Figure 2e, right panel). In fact, a deletion mutant containing only the central domain (MDM4 106–360) also stabilized GFP-HIPK2 (Figure 2f, densitometric values under the blot) whereas a MDM4 mutant lacking the central domain (MDM4BD+RF) failed to do this (Figure 2g), indicating that direct binding between the two proteins is required for HIPK2 stabilization.

HIPK2 mediates MDM4-induced phosphorylation of $p53Ser46^P$

Previous data indicate that MDM4 binds and stabilizes HIPK2. To establish whether HIPK2 mediates the MDM4 activity towards $p53Ser46^P$, MDM4-mediated regulation of $p53Ser46^P$ was analysed following depletion of HIPK2 (si*HIPK2*). At 5 h after Adr treatment, when the binding between MDM4 and p53 is still present,[20,29] the decrease of $p53Ser46^P$ and cell apoptosis by knockdown of MDM4 was abolished by si*HIPK2* (Figures 3a–c). indicating that the presence of HIPK2 is indeed required for MDM4 activity. Analogously, the effects of overexpressed MDM4 were abolished by siHIPK2 (Figures 3d–f).

To further analyse the role of MDM4/HIPK2 relationship in the MDM4-mediated induction of $p53Ser46^P$, it was compared the ability of the MDM4 deletion mutants that bind p53 (MDM4BD +RF) or HIPK2 (MDM4ΔBD), to promote $p53Ser46^P$. As previously observed, the expression of wt-MDM4 in $Mdm4^{-/-}p53^{-/-}$ MEFs caused a robust increase of total p53[5,7,30] and an even higher increase of $p53Ser46^P$, in comparison to the sole expression of high amount of p53 (3X)[9] (Figure 3g, densitometric values under the blot). Western blot (WB) of overexpressed wtp53, p53S46A and p53S46D confirmed the specificity of $p53Ser46^P$ induction due to the overexpression (Supplementary Figure 1h). In comparison, MDM4BD+RF, which binds p53 but not HIPK2, did not stimulate p53Ser46 phosphorylation despite the increase of total p53 levels (Figure 3g), this suggesting that the HIPK2 stabilization mediated by MDM4 is necessary for the increase of $p53Ser46^P$. Unexpectedly, the MDM4ΔBD mutant that binds HIPK2 but not p53, did not increase $p53Ser46^P$levels, indicating that HIPK2 stabilization by MDM4 is not sufficient to promote p53Ser46 phosphorylation and suggesting that the binding of MDM4 to both HIPK2 and p53 is necessary. MDM4ΔBD and MDM4 containing only the p53-binding domain (MDM4BD) behaved similarly to the other mutants and even reduced $p53Ser46^P$ in comparison to p53 3X (Figure 3g, densitometric values under the blot). This may be due to their ability to bind/sequester HIPK2 and p53 and prevent their functional association supporting previous results. According to molecular data, the highest levels of cell death to cisplatin-induced DNA damage were conferred by wt-MDM4, whereas the mutants were unable to induce significant levels of cell death (Figure 3h), supporting the role of full-length MDM4 in promoting p53/HIPK2 apoptotic function during DNA damage.

Since endogenous murine Hipk2 is not currently detectable in MEFs,[31] to further support previous data HIPK2-p53 binding was analysed in the absence or presence of MDM4. The presence of MDM4 increased the binding of GST-HIPK2 to p53 by *in vitro* assay (Figure 3i). Similarly, upon Adr treatment overexpression of MDM4 resulted in increased association of itself and of HIPK2 to p53 concurrent with increased levels of $p53Ser46^P$, confirming that MDM4 enhances the functional association between HIPK2 and p53 (Figure 3j).

Dissociation of MDM4 from MDM2 allows MDM4 activity

Previous data support a model in which MDM4 by binding and preventing HIPK2 degradation, facilitates the association and

Figure 1. MDM4 regulates HIPK2 protein levels. (**a**) Western blot (WB) of the indicated proteins in MCF10A cells transfected with 20 nM stealth *MDM4*-specific (si*MDM4*) or stealth control RNA (si*CTL*) for 48 h and exposed to 2 μM Adr for the indicated time points. Ratio of densitometric values of p53Ser46P to p53 total levels is shown at the bottom of the blot. p53Ser46P/p53Tot ratio in siCTL-treated cells was arbitrarily set to 1. (**b**) Upper panel: WB of the indicated proteins in $p53^{+/+}$ and $p53^{-/-}$HCT116 cells transfected with si*CTL* or si*MDM4*. Ratio of densitometric values of HIPK2 to tubulin is shown at the bottom of the blot. HIPK2/TUB ratio from control lane was arbitrarily set to 1. Lower panel: RTqPCR of *HIPK2* mRNA normalized to h*TBP*. *HIPK2* mRNA expression levels of si*CTL* cells were arbitrarily set to 1. (**c**) WB of the indicated proteins in MCF10A-tet-shMDM4 cells treated or untreated for 48 h with doxycycline, and collected at 24 h after infection with Adenoviral vector carrying MDM4 cDNA (AdMDM4) or an empty Adenoviral vector. Analysis of HIPK2 levels as in **b**. (**d**) WB of the indicated proteins in $Mdm4^{-/-}p53^{-/-}$ MEFs transfected with the indicated expression vectors. Analysis of HIPK2 levels as in **b**. (**e**) WB of the indicated proteins in MCF10A cells transfected with si*CTL* or si*MDM4* and treated with 25 μM Mg132 for 8 h. Analysis of HIPK2 levels as in **b**. (**f**) HCT116 cells transfected for 48 h with GFP-HIPK2 alone (CTL) or in combination with pcDNA3.1-MDM4 and treated with cycloheximide (CHX, 50 μg/ml). WCE were collected at the indicated time points and analysed by WB (left panel). Densitometric analysis of GFP-HIPK2 levels is shown in the right panel. HIPK2 bands intensity was normalized to Tubulin, then normalized to the $t = 0$ value, set to 100%. (**g**) U2OS cells transfected as in **a** and at 24 h treated with cycloheximide (CHX, 70 μg/ml). WCE were collected at the indicated time points and analysed by WB (left panel). Analysis of HIPK2 levels (right panel) as in **f**.

activity of this kinase towards p53. HIPK2 degradation is carried out by the ubiquitin ligase MDM2.[24] Current model suggests that majority of MDM4 is associated to MDM2, promoting its degradative activity towards p53.[1] We therefore analysed the association between MDM4 and MDM2 under these conditions. The two proteins were co-immunoprecipitated at different time points after Adr treatment, using as control a cytostatic dose of Adr which causes a growth arrest (GA), a condition that maintains the association of two proteins.[32,33] Noteworthy, a strong decrease in MDM4/MDM2 association was evident at the dose of Adr that causes an apoptotic response (AP), whereas the association persisted at the cytostatic dose (GA) (Figure 4a, right panel). Dissociation occurred quite early before any change in the levels of the two proteins appeared. Analysis of primary human

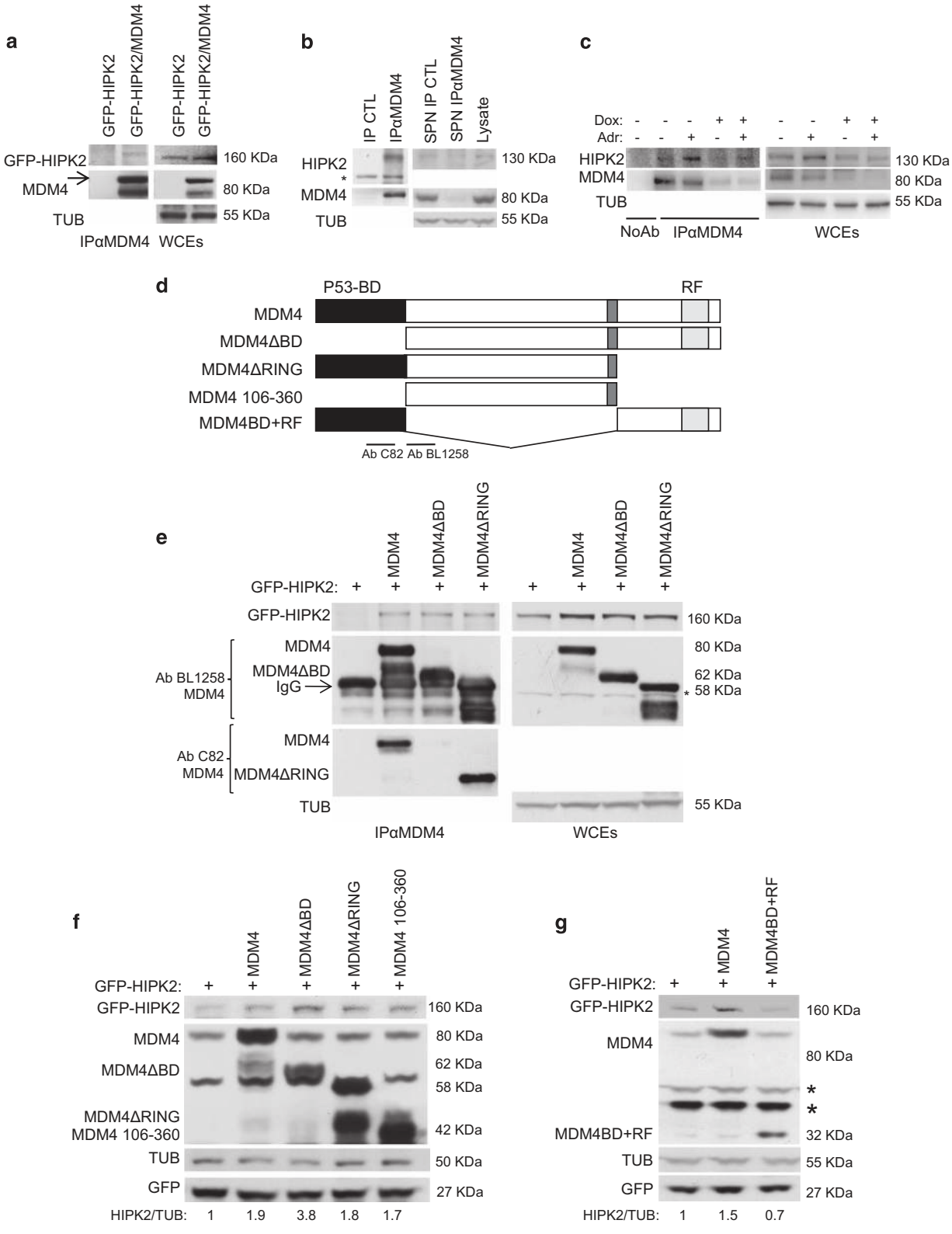

mammary cells, HMEC, confirmed these data (Supplementary Figures 2a and b) independently of the levels of MDM4, MDM2 and p53 in this cell line compared with MCF10A (Supplementary Figure 2c). These results suggest that dissociation of MDM2 from MDM4 allows MDM4 to promote HIPK2 activity.

To ascertain that MDM4/MDM2 association interferes with MDM4 binding to HIPK2, we analysed MDM4/HIPK2 association in the presence or absence of MDM2. Overexpression of MDM2 caused its association to MDM4 and the dissociation of HIPK2 (Figure 4b) independently of protein degradation as assessed by MG132 treatment (Figure 4c, Supplementary Figure 2d). To further support these data, MDM2 antagonized MDM4-mediated stimulation of p53Ser46^{P} and reduction of cell viability in *Mdm4*$^{-/-}$*p53*$^{-/-}$ MEFs, whereas it was ineffective towards MDM4C437G, a mutant MDM4 unable to bind MDM2 (Figures 4d and e). Accordingly, MDM2 expression coincided with a ladder of MDM4 but not of MDM4C437G ubiquitinated forms. These data confirm that the dissociation of the two proteins allows the realization of MDM4 activity towards HIPK2/p53.

Proteomic and bioinformatics analysis of MCF10A cells

P53Ser46^{P} is a modification involved both in the mitochondrial as well as in the transcriptional activity of p53 towards activated and repressed targets. In order to verify which of these p53 functions was mostly affected by MDM4, we evaluated proteomic profile of MCF10A in the presence or absence of MDM4 and Adr. si*MDM4*-MCF10A or control si*CTL*-MCF10A were untreated or treated with Adr for 5 h and protein extracts were subjected to a comparative proteomic analysis. Preliminary WB of these fractions confirmed the reduction of MDM4, HIPK2 and p53Ser46^{P} levels as previously reported (Supplementary Figure 3a). Cytoplasmic extracts were analysed through a label-free data-independent differential proteomic assay by nUPLC-MS^{E}, which allows quantitative assessment of changes between samples with high precision[34] (Supplementary Figure 3b). Proteomic analysis identified 72 proteins significantly differentially expressed between si*MDM4*-MCF10A and si*CTL*-MCF10A exposed to Adr (Supplementary Tables 1 and 3). Unbiased bioinformatics meta-analysis of these proteins with Ingenuity Pathway Analysis (IPA) displayed three main molecular networks affected by MDM4 depletion (Supplementary Table 5). Of note, two of these (one of which involving p53) relate to cell death, indicating that MDM4 depletion alters the proteome associated to this cellular condition. Association of the protein data set to biological functions (by IPA functional analysis) confirmed a significant alteration of 'cell death' function with the highest number of proteins altered by MDM4 depletion, belonging to this group (Supplementary Table 6). In the absence of Adr, comparative proteomic analysis between si*MDM4*-MCF10A and si*CTL*-MCF10A showed 42 proteins differentially expressed (Supplementary Tables 1 and 2). Comparison between this data set and the previous one showed low overlapping (Figure 5a), suggesting that MDM4 impacts different protein pools depending on cell growth conditions. IPA-Functional analysis indicated that the highest number of altered proteins in untreated cells (si*MDM4*-MCF10A vs si*CTL*-MCF10A) belongs to 'Cellular Growth and Proliferation' function (Supplementary Table 6) in agreement with the inhibitory function of MDM4 towards cell proliferation.[28]

To gain insight into MDM4 activity, the profile of proteins altered by MDM4 depletion upon Adr treatment was compared with that of proteins altered by Adr treatment *per se* (as resulting from comparison of si*CTL*+Adr vs si*CTL* cells). Adr caused a significant change of 71 protein levels most of which (50/71) were downregulated (Supplementary Tables 1 and 4). This matches previous microarray transcriptional analyses reporting a decrease of cell transcription in the early phase of apoptosis.[35–37] Under these conditions, MDM4 depletion altered 37 out of 71 proteins affected by Adr (Figure 5b). Thirty-five out of these 37 were oppositely regulated by si*MDM4* (Figures 5b and d). Specifically, si*MDM4* caused upregulation of 26/35 proteins downregulated by Adr treatment, suggesting that MDM4 is required for the decrease of these molecules (Figure 5d). The inability of shotgun analysis to detect low abundance proteins was responsible for the absence of HIPK2 in this data set. Comparison of the three protein pools confirmed low overlapping with untreated cells (Figure 5c).

Analysis focused on the p53-related network confirmed previous observations: 8/10 proteins decreased by Adr (Figure 5e, green symbols) were upregulated in si*MDM4* cells (Figure 5f, red symbols). Of note, p53 and HIPK2 directly repress some of these molecules (ITGB4, LGALS3 and SOD2),[17,18,38] that share an anti-apoptotic activity, a feature common to other proteins downregulated by Adr (P4HB, KRT5, KRT8 and S100A11). Overall, these data indicate that: (i) in the first hours of DNA damage response there is a widespread downregulation of proteins, many of which with a common anti-apoptotic activity; (ii) some of these proteins are targets of p53/HIPK2 transcriptional repressive activity; (iii) MDM4 is involved in the downregulation of these targets supporting its function in promoting p53/HIPK2 activity (Supplementary Table 3).

MDM4 enhances p53-mediated repression of anti-apoptotic proteins

To validate proteomic data, WB analysis of cytoplasmic cell extracts from independent experiments was performed. The levels of p53 targets galectin-3 (LGALS3), integrin-beta4 (ITGB4) and superoxide dismutase-2 (SOD2) were indeed downregulated by Adr treatment, and si*MDM4* resulted in complete recovery of such downregulation (Figure 6a). WB analysis of the cytoplasmic cell extracts used for nUPLC-MS^{E} confirmed these results (data not shown). A time course of these proteins in whole cell extract (WCE) confirmed a marked downregulation of LGALS3, ITGB4 and SOD2 levels at 16 h, ruling out that these effects are due to subcellular relocalization

Figure 2. MDM4-mediated stabilization of HIPK2 depends on their association. (**a**) *Mdm4*$^{-/-}$*p53*$^{-/-}$ MEFs were transfected with the indicated plasmids and immunocomplexes were analysed after immunoprecipitation of 500 μg of WCE with anti-MDM4 antibody BL1258 (IPαMDM4, left panel). Right panel shows WB analysis of 1/10 of WCEs. (**b**) Analysis of co-immunocomplexes in MCF10A by immunoprecipitation of 2 mg of WCE with anti-MDM4 antibody BL1258 (IPαMDM4) or nonspecific IgG (IP CTL; left panel). Right panel shows WB analysis of 1/50 of WCEs (lysate). SPN IP CTL and SPN IPαMDM4 indicate supernatant of control and MDM4 immunoprecipitated samples, respectively. Asterisk (*) represents a nonspecific band. (**c**) Analysis of co-immunocomplexes in MCF10A-tet-shMDM4 cells treated or untreated for 24 h with doxycycline and treated with Adr for 2 h. Eight hundred micrograms of WCE were immunoprecipitated with anti-MDM4 antibody C82 (IPαMDM4). Right panel shows WB analysis of 1/20 of WCEs (lysate). (**d**) Scheme of MDM4 deletion mutants used in **e**–**g**. BD means p53-binding domain, RF Ring Finger domain. Underneath lines indicate the two different MDM4 antibodies used to detect deletion mutant (AbC82; AbBL1258). (**e**) *Mdm4*$^{-/-}$*p53*$^{-/-}$ MEFs were transfected with the indicated plasmids and immunocomplexes analysed after immunoprecipitation of 500 μg of WCE with anti-MDM4 antibodies (IPαMDM4, left panel). The antibodies used in the WB are shown. AbC82 was used to detect MDM4ΔRING, masked by IgG in AbBL1258 blot. Right panel shows WB analysis of 1/10 of WCEs. Asterisk (*) indicates a nonspecific band. (**f** and **g**) WB of the indicated proteins in HCT116 cells transfected with the indicated plasmids. Ratio of densitometric values of HIPK2 to Tubulin is shown at the bottom of the blot. HIPK2/TUB ratio from control lane was arbitrarily set to 1.

(Supplementary Figures 4a and b). As previously observed, si*MDM4* reversed this decrease, confirming the requirement of MDM4 for these molecules' downregulation. This occurs even at 16 h when MDM4 levels are reduced (Supplementary Figure 4a), supporting the hypothesis that MDM4 acts modifying upstream factors involved in this decrease, such as HIPK2. Downregulation of these

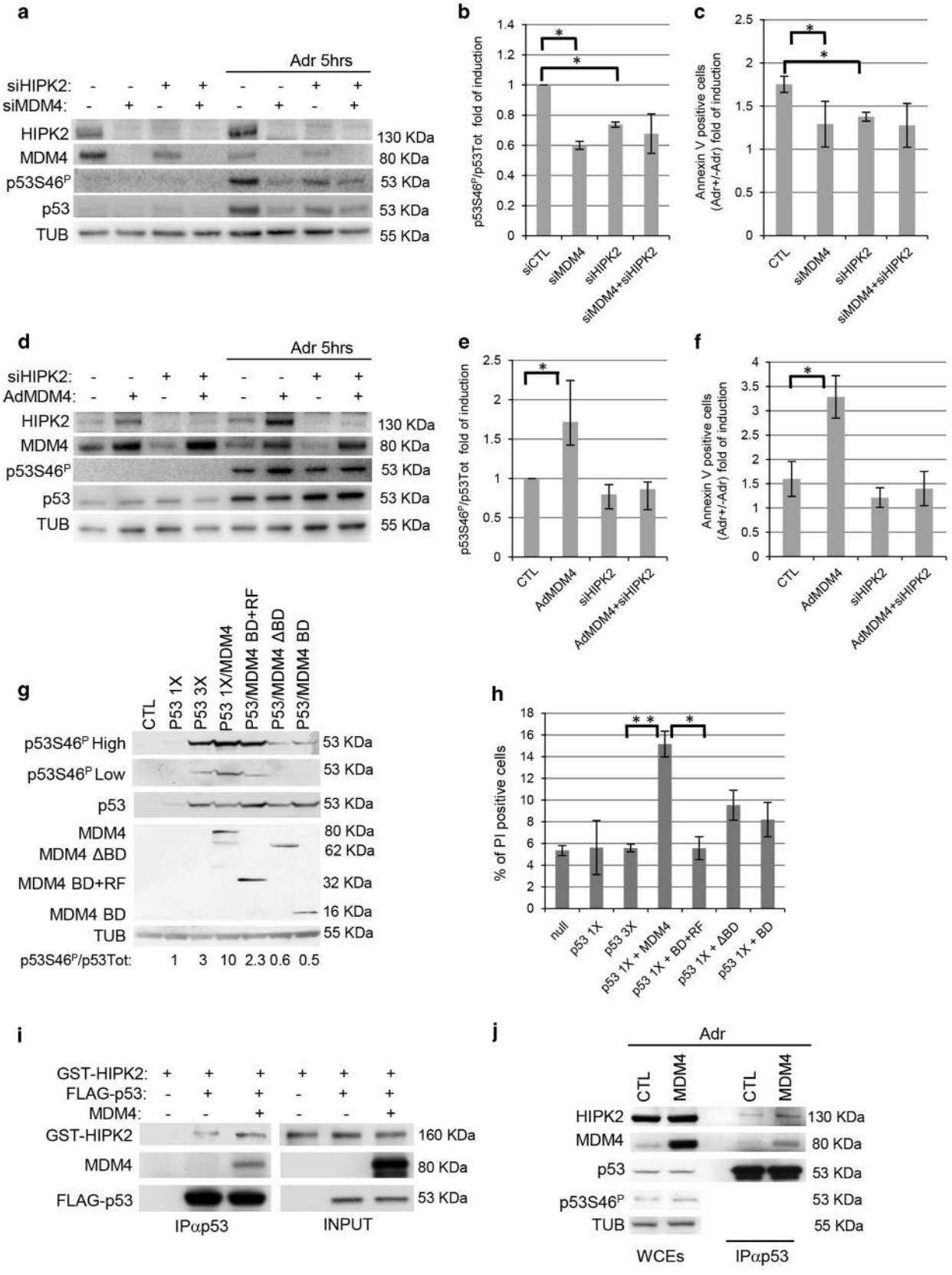

targets by Adr and the effects of MDM4 depletion were confirmed in other cell lines (Supplementary Figure 5a).

RT–qPCR evidenced that upon Adr treatment, all three transcripts undergo a consistent and persistent decrease which was counteracted by depletion of MDM4, although with different efficiency (Figure 6b). In comparison, transcriptional activation of proapoptotic genes, *NOXA* and *BAX*, was not significantly altered by *siMDM4* (Supplementary Figure 4c). Stable interference of p53 in MCF10A (pSuper.retro-ip53) (Supplementary Figures 4d and e) prevented the decrease of these proteins in comparison to control MCF10A (pSuper.retro-iSC) (Figure 6c). Of note, depletion of MDM4 did not affect the levels of these proteins in the ip53 cells whereas it was effective in control cells (Figure 6c) indicating that the regulation of *LGALS3*, *ITGB4* and *SOD2* by MDM4 requires the presence of p53. RT–qPCR further confirmed these data (Figure 6d). Analysis of promoter occupancy by p53 through ChIP showed increased recruitment of p53 at the promoter of *LGALS3* following Adr treatment, antagonized by MDM4 depletion (Figure 6e, Supplementary Figure 5b). Overall, these data demonstrate that MDM4 promotes p53-mediated transcriptional repression of *ITGB4*, *LGALS3* and *SOD2* induced by DNA damage.

To confirm that this occurs also *in vivo*, C57Bl6 female mice were treated with a sublethal dose of γ-irradiation (6 Gy) and the levels of murine p53, HIPK2 and LGALS3 were analysed in mammary fat pad samples at different time points. As evidenced by WB, p53 levels markedly increased after 6 h whereas LGALS3 levels decreased correspondingly (Figure 6f, Supplementary Figure 6a). The appearance of PARP cleaved form p85 confirmed the apoptotic features of these samples (Supplementary Figure 6a). Immunohistochemistry showed a strong signal for LGALS3 and the characteristic nuclear punctate signal for HIPK2[39] in the luminal cells of breast ducts (Figure 6g, Supplementary Figure 6d). LGALS3 signal progressively decrease whereas that of HIPK2 increased along time-course irradiation (Figures 6g and h). Of note, HIPK2 levels were significantly increased in γ-irradiated Mdm4-overexpressing mice ($Mdm4^{Tg/+}$)[40] compared with age-matched control mice (WT); conversely, those of LGALS3 were decreased (Figure 6i, Supplementary Figures 6b–d). Basal levels of LGALS3 were not affected by the presence of the transgene (data not shown). Overall these data confirm the downregulation of LGALS3 in breast tissue following DNA damage and the ability of MDM4 to promote such downregulation and increase HIPK2 levels.

MDM4 acts at the cytoplasmic level

Previous data point to MDM4 as a proapoptotic factor preceding and promoting transcriptional repressive activity of p53/HIPK2 during the early DNA damage response. To confirm that MDM4 activity occurs in the cytoplasm preceding nuclear activity of p53/HIPK2, we analysed the two subcellular compartments in the presence or absence of MDM4. Co-expression of GFP-HIPK2 and MDM4 in MEFs resulted in increased cytoplasmic localization of HIPK2 compared with the sole expression of HIPK2 (Supplementary Figure 7), indicating that MDM4 increases HIPK2 cytoplasmic localization. Protein analysis of subcellular fractions confirmed that si*MDM4* caused a stronger decrease of HIPK2 levels in the cytoplasmic compared with the nuclear fraction (Figure 7a). $P53Ser46^P$ levels were also strongly decreased, whereas those of p53 were less affected. As it has been reported that activated p53 shuttles rapidly from cytoplasm to the nucleus,[41] to ascertain that MDM4-mediated phosphorylation of p53Ser46 does indeed occur in the cytoplasm, we blocked p53 shuttling by downregulating importin-α3 (*KPNA4*) which mediates p53 nuclear translocation. Si*KPNA4* reduced the nuclear pool of p53 and, even more markedly, that of $p53Ser46^P$ while increasing the cytoplasmic one (Figure 7b, compare lane 3 with 1 in each panel, densitometric values under the blot), supporting the hypothesis that this modification occurs primarily in the cytoplasm. Of note, under these conditions depletion of MDM4 did not modify nuclear $p53Ser46^P$ levels, but decreased the cytoplasmic levels (Figure 7b, compare lane 4 with 3 in each panel, densitometric values under the blot). In agreement with cytoplasmic retention of the repressor p53, interference of importin-α3 highly increased the levels of LGALS3 and ITGB4 proteins (Figure 7b, compare lane 3 with 1 in each panel). Strikingly, block of p53 nuclear import caused the inefficacy of si*MDM4* to upregulate these proteins—despite the decrease of cytoplasmic $p53Ser46^P$—whereas si*MDM4* was still effective in control cells. These data confirm that MDM4-mediated increase of $p53Ser46^P$ occurs in the cytoplasm preceding repressive transcriptional activity of p53/HIPK2.

DISCUSSION

In this work, we have addressed the role of MDM4 in the phosphorylation of p53 at Ser46 and in the cell response associated to this modification. Our data demonstrate that MDM4 directly stimulates this phosphorylation by promoting functional association between HIPK2 and p53 and that this modification is involved in a coordinated repressive activity of p53/HIPK2 in the early DNA damage response.

Particularly, the enhancement of $p53Ser46^P$ by MDM4 is related to the increased stability of homeodomain-interacting protein kinase 2 (HIPK2). HIPK2 is a member of nuclear Ser/Thr kinase family originally identified as corepressor for homeodomain transcription factors.[42] It activates p53-dependent transcription and apoptosis by phosphorylating human p53 at Ser46.[16,39,43–45] This phosphorylation promotes p53 acetylation responsible for transcriptional activation of proapoptotic targets.[16,46] Our data add one more piece to the p53/HIPK2 connection by enlightening the role of HIPK2 corepressive activity in the severe DNA damage response. These data complement previous findings that MDM4 facilitates p53-mediated mitochondrial apoptosis by enhancing

Figure 3. HIPK2 mediates MDM4 activity. (**a**) WB of the indicated proteins in MCF10A cells transfected with 40 μM stealth *HIPK2*-specific (si*HIPK2*) or stealth control RNA (si*CTL*). At 72 h, cells were exposed to 2 μM Adr for 5 h. (**b**) Densitometric values of $p53Ser46^P$ to p53 total levels. $P53Ser46^P$/p53Tot ratio from control lane was arbitrarily set to 1.Mean ± s.d. of three independent experiments is shown (*$P < 0.05$ Student's *t*-test). (**c**) Ratio of Adr-treated (8 h) AnnexinV-positive cells to untreated cells. Mean ± s.d. of three independent experiments is shown. (**d**) WB of the indicated proteins in MCF10A cells transfected with 40 μM stealth *HIPK2*-specific (si*HIPK2*) or stealth control (si*CTL*) RNA. At 48 h, cells were infected with AdMDM4 or empty adenoviral vector and at additional 24 h exposed to 2 μM Adr for 5 h. (**e**) and (**f**) Graphs as in **b** and **c**. (**g**) WB analysis of $Mdm4^{-/-}p53^{-/-}$ MEFs transfected with indicated plasmids for 18 h. CTL indicates pcDNA3.1 control vector. 'High' and 'low' represent different exposures. Ratio of densitometric values of $p53Ser46^P$ to p53 total levels is shown at the bottom of the blot. $p53Ser46^P$/p53Tot ratio of p53 1X was arbitrarily set to 1. (**h**) Percentage of PI-positive cells transfected as in **g** and treated with 5 μM cisplatin for 18 h. Mean ± s.d. of three independent experiments is shown (**$P < 0.01$; *$P < 0.05$ Student's *t*-test). (**i**) Analysis of *in vitro* p53 immunocomplexes by using *in vitro* translated proteins MDM4, GST-HIPK2 and FLAG-p53. *In vitro* translated proteins were incubated in Saito's modified buffer for 2 h under gently shaking at 4 °C. P53 was immunoprecipitaed using anti-p53 antibodies 1C12-Ab421. Right panel shows WB of the INPUT proteins. (**j**) MCF10A cells transfected with pcDNA3.1 control vector (CTL) or pcDNA3.1MDM4 vector (MDM4) and treated with Adr for 5 h. Immunocomplexes were analysed after immunoprecipitation of 2 mg of WCE with anti-p53 antibodies 1C12-Ab421 (IPαp53). Left part shows WB analysis of 1/50 of WCE (lysate).

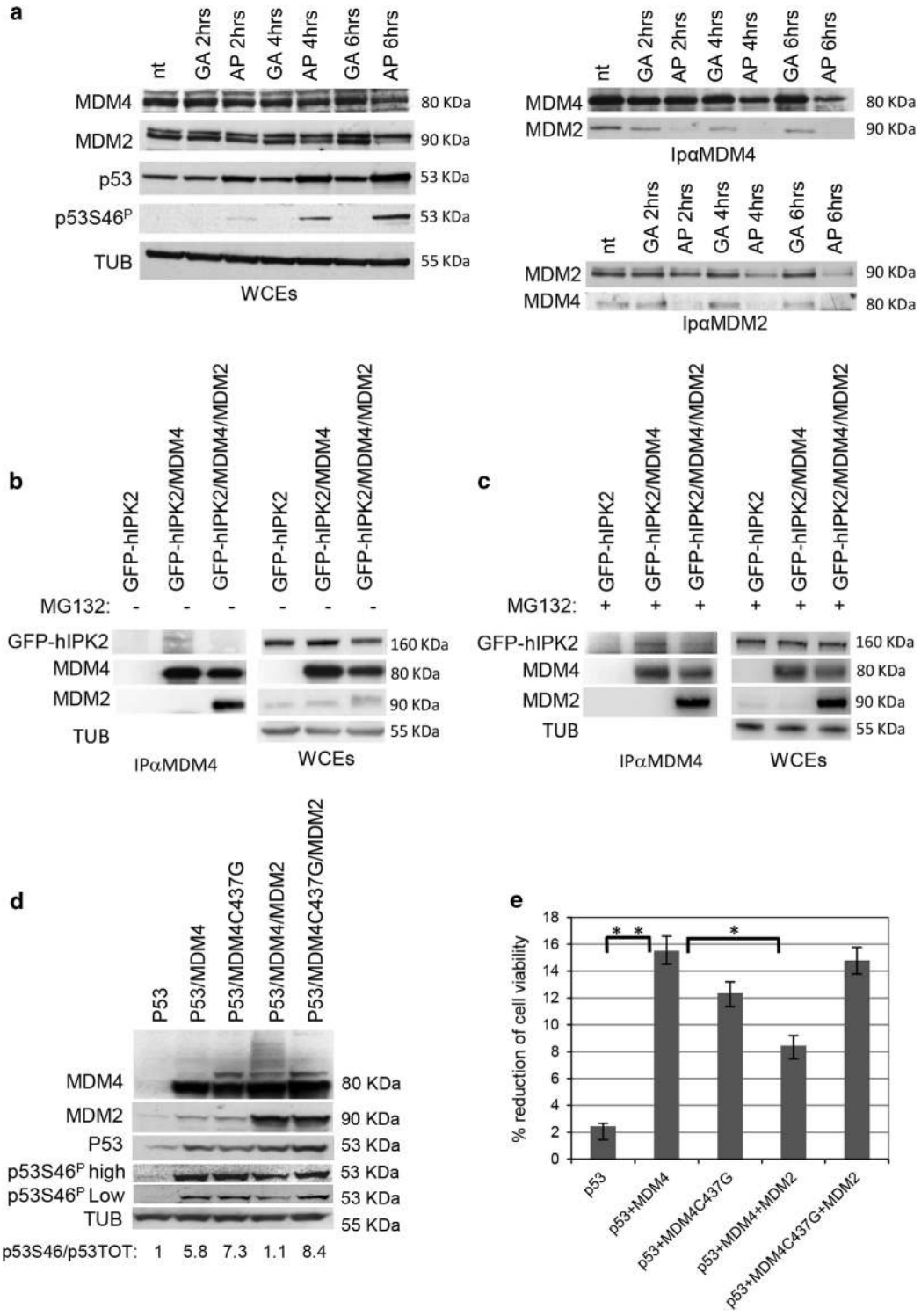

Figure 4. MDM4 dissociates from MDM2 and promotes HIPK2/p53 functional interaction. (**a**) Western blot of the indicated proteins in WCEs and in co-immunoprecipitations (IP) of MCF10A cells untreated (nt) or treated with adriamycin (0.2 μM = GA) and (2 μM = AP) at the indicated time points. Immunoprecipitation were performed with anti-MDM4 antibody BL1258 (IPαMDM4, upper panel) and anti-MDM2 antibodies 2A10/Ab1 (IPαMDM2, lower panel). (**b** and **c**) Immunocomplexes of *Mdm4*$^{-/-}$*p53*$^{-/-}$ MEFs transfected with the indicated plasmids (**b**) and treated with 20 μM MG132 for 6 h (**c**). Five hundred micrograms of WCE were immunoprecipitated with anti-MDM4 antibody BL1258 (IPαMDM4, left panels). (**d**) WB analysis of *Mdm4*$^{-/-}$*p53*$^{-/-}$ MEFs transfected with indicated plasmids. Ratio of densitometric values of p53Ser46^{P} versus p53 total levels is shown at the bottom of the blot. p53Ser46^{P}/p53Tot ratio from p53 was arbitrarily set to 1. (**e**) Viability by cell titre blue colorimetric assay of cells transfected as in **d**. Columns represent % of reduction of cell viability in comparison with cells transfected with control vector. Mean ± s.d. of two experiments in octuplicate are shown (**$P < 0.01$; *$P < 0.05$ Student's *t*-test).

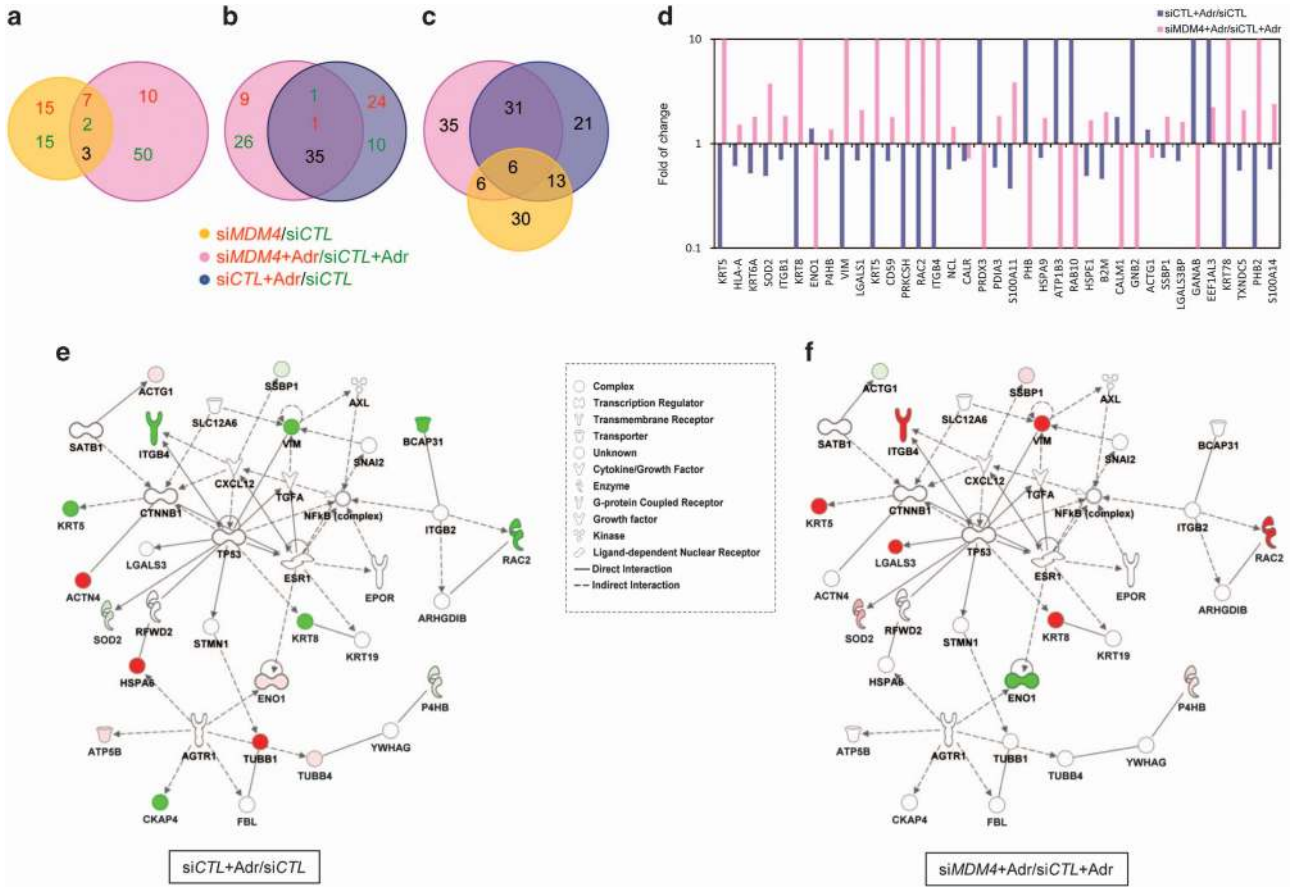

Figure 5. Shotgun proteomic and bioinformatic analysis of MCF10A cells. (**a**) Overlap of proteins resulting from comparison of si*MDM4*-MCF10A vs siCTL-MCF10A cells (yellow circle) with those resulting from si*MDM4*-MCF10A+Adr vs si*CTL*-MCF10A+Adr cells (pink circle). Adriamycin (Adr) 2 μM was administered for 5 h. Red numbers represent upregulated proteins; green numbers represent downregulated proteins; black number in the intersection represents proteins regulated in an opposite manner. Protein hits were filtered to a fold difference larger than 30% (corresponding to a ratio of (+) > 1.3 or (−) < 0.7) (**b**) Overlap of proteins resulting from comparison of si*MDM4*-MCF10A+Adr vs si*CTL*-MCF10A+Adr (pink circle) with those resulting from si*CTL*-MCF10A+Adr vs si*CTL*-MCF10A cells (blue circle). Colour numbers are represented as in **a**. (**c**) Overlap of the three groups represented in **a** and **b**. Black numbers represent modulated proteins. (**d**) Fold of change of indicated proteins resulting from comparison of si*MDM4*-MCF10A+Adr vs si*CTL*-MCF10A+Adr (pink columns) with those resulting from si*CTL*-MCF10A+Adr vs si*CTL*-MCF10A cells (blue columns). Values are in a logarithmic scale. (**e** and **f**) P53 networks identified from IPA core analysis. Continued and dotted lines represent respectively direct and indirect interactions. (**e**) Red and green proteins are respectively significantly upregulated and downregulated by Adr (as resulted from si*CTL*-MCF10A+Adr vs si*CTL*-MCF10A). (**f**) Red and green proteins are upregulated and downregulated by *siMDM4* in the presence of Adr (as resulted from si*MDM4*-MCF10A+Adr vs si*CTL*-MCF10A+Adr), respectively. Dark colours indicate highly represented proteins. Shapes in the legend indicate different functions of the network proteins.

p53Ser46^{P},[9,11,47] and suggest p53Ser46^{P} as an early common signature of p53-mediated transcription-dependent and -independent apoptosis.

Mechanistically, we demonstrated that upon DNA damage, cytoplasmic MDM4 dissociates from MDM2 and binds HIPK2 promoting its stabilization and functional interaction with p53. These data are the evidence of a dynamic behaviour of the heterodimer and provide a molecular explanation for the distinct activities of MDM4 in different cell growth conditions.[48] Interestingly, this dissociation does not occur in breast tumour cell line MCF7 (data not shown) suggesting one possible mechanism of impairment of MDM4 proapoptotic activity in tumour cells. In addition, the different ratio of MDM4/MDM2 levels may further contribute to impair MDM4 activities.[48] The MDM4-mediated HIPK2/p53 activation precedes p53/HIPK2 repression of targets that share a common anti-apoptotic activity. The targets identified by proteomic analysis are non-canonical anti-apoptotic proteins although a canonical anti-apoptotic protein such as Bcl2, behaved similarly to these proteins (data not shown). Although the relevance of these proteins in the global apoptotic response has not been elucidated, these results raise the hypothesis of a diffuse barrier to cell death in epithelial breast cells, this being removed before an irreversible apoptotic outcome occurs. Accordingly, the presence of an apoptotic threshold determined by the relative levels of apoptotic and anti-apoptotic factors has been demonstrated.[49] Of note, some of these proteins (LGALS3, ITGB4, AnnexinA1 and S100A11) are often upregulated in human cancer and even used as diagnostic marker (LGALS3), underscoring their importance in cell biology.[50–54] Interestingly, their overexpression has been considered a way for cancer cells to escape cell death induced by DNA-damaging anti-cancer drugs.[52,53,55]

These data support the cytoplasm as an important cell compartment for death choice, including that affected by p53. In line with this model, recent data demonstrated that accumulation and activation of p53 in the cytoplasm precedes and contributes to nuclear p53 activation.[41] P53-mediated transcriptional activation of apoptotic targets has been linked to the formation of nuclear Axin-based p53 complexes that in addition to Ser46 phosphorylation promote Tip60-mediated p53 acetylation at lysine K120.[56–58] Our data raise the hypothesis of a cytoplasmic scaffold constituted by MDM4 that favours HIPK2/p53 assembly, similarly to the assembly of cytoplasmic

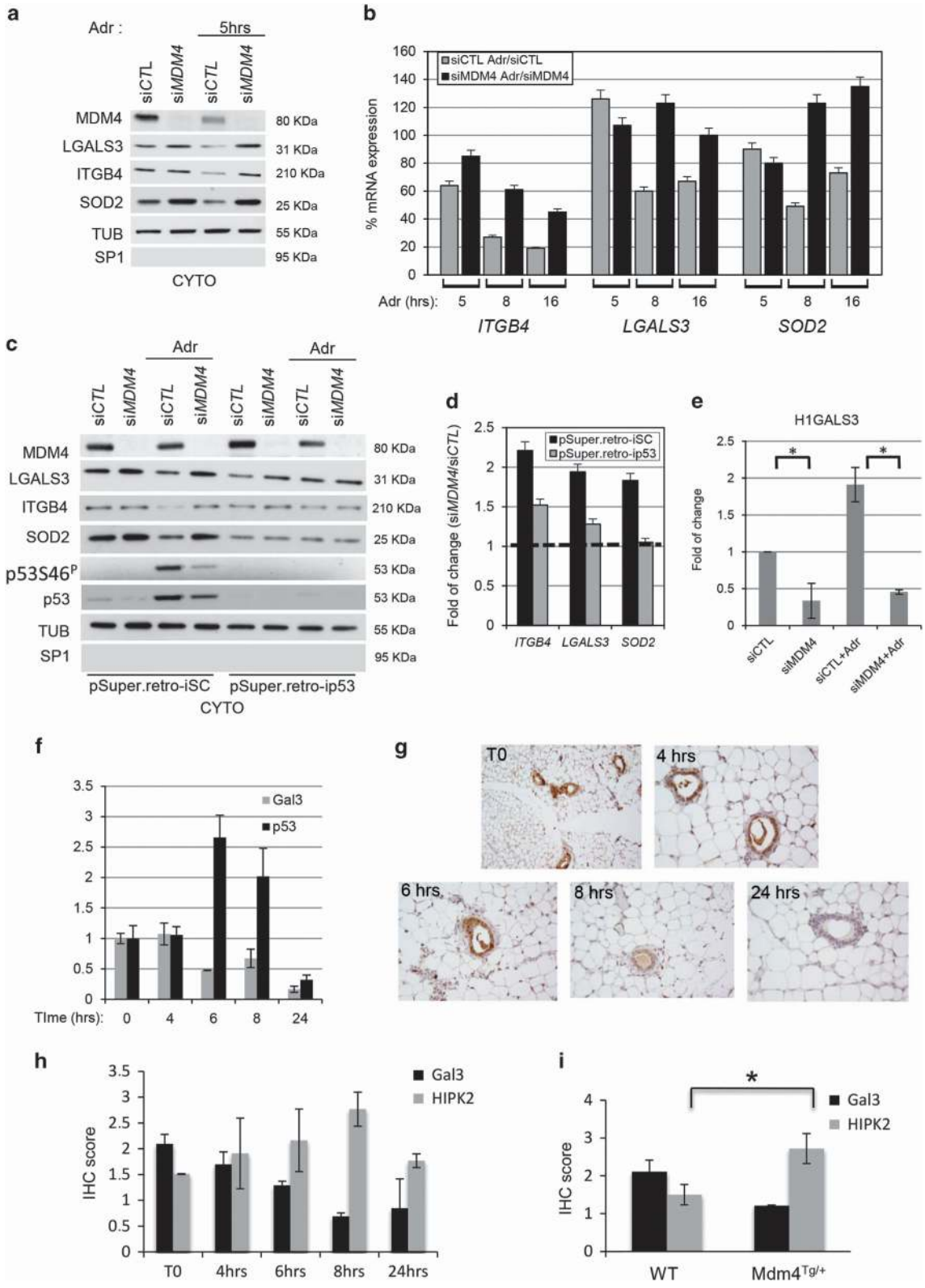

death-inducing signalling complexes that constitute an important step in the execution of programmed cell death.[59] The existence of nuclear and cytoplasmic complexes able to stimulate the same p53 modification, that is Ser46^{P}, may indicate the presence of overlapping pathways to ensure the proper realization of a crucial process as the apoptosis. Alternatively, different complexes might join different molecules to perform post-translational signatures with different activities. However, at present, it is not known whether p53 repressive activity requires modifications other than p53Se46^{P}.

Noteworthy, these results suggest that mislocalization of proteins involved in this process may represent a further way

Figure 6. MDM4 enhances p53-mediated repression of anti-apoptotic proteins. (**a**) WB of the indicated proteins in cytoplasmic extracts (CYTO) of si*MDM4*-MCF10A or si*CTL*-MCF10A cells untreated or treated with 2 μM Adr for the indicated time point. (**b**) RT–qPCR of mRNA expression of the indicated genes in si*CTL*-MCF10A (grey columns) and si*MDM4*-MCF10A cells (black columns) exposed to Adr for the indicated time points. Gene activation was calculated by setting 100% gene expression in untreated cells of each MCF10A population. Mean ± s.e.m. of two experiments performed in triplicates are shown. (**c**) WB of the indicated proteins in CYTO of pSuper.retro-iSCMCF10A and pSuper.retro-ip53MCF10A cells interfered with si*CTL* or si*MDM4* and exposed to 2 μM Adr for 8 h. (**d**) RT–qPCR of mRNA of the indicated genes in pSuper.retro-iSCMCF10A and pSuper.retro-ip53MCF10A cells exposed to Adr. Gene expression in si*MDM4* and si*CTL* cell populations was normalized to the gene expression in untreated cells. Columns represent the ratio of each normalized gene in pSuper.retro-iSCMCF10A (black columns) and pSuper.retro-ip53MCF10A (grey columns) cells. Dotted line indicates unchanged gene expression. (**e**) ChIP analysis of p53 binding on *LGALS3* promoter in HCT116 cells transfected with si*CTL* and si*MDM4* and treated with 2 μM Adr for 16 h. Mean ± s.d. of three experiments are shown (**P* = 0.05 Student's *t*-test). (**f**) Densitometric analysis of WB of indicated proteins in breast tissue isolated at different time points from female mice subjected to total body γ-irradiation (6 Gy). Two animals were sacrificed at each time point. Mean ± s.d. from two animals are shown. (**g**) Immunohistochemistry of mLgals3 expression in mammary fat pad samples of γ-irradiated mice as in **f**. (**h**) Immunohistochemistry evaluation of mLgals3 and Hipk2. Immunohistochemistry score was obtained by multiplying the percentage of positive cells by the intensity (staining intensity was scored on a scale of three grades: 1, weak staining; 2, moderate staining; 3, strong) in five ducts/sample. Four mammary fat pad samples/mouse were analysed. Mean ± s.d. from two animals are shown. (**i**) Analysis of mLgals3 and Hipk2 score calculated as in **h**. Four mammary fat pad samples/mouse were analysed. Mean ± s.d. from two control (WT) and two Mdm4-overexpressing transgenic ($Mdm4^{Tg/+}$) mice are shown (**P* = 0.05 Student's *t*-test).

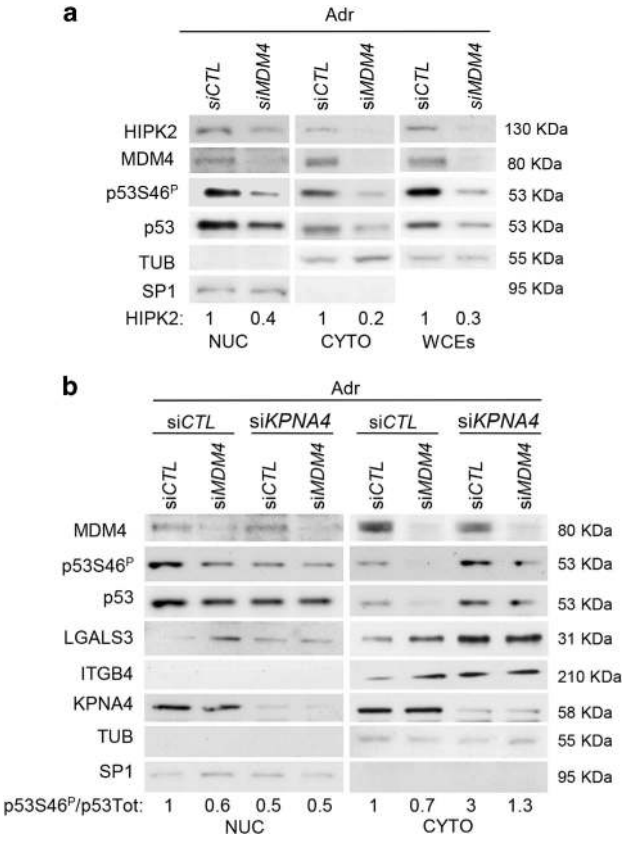

Figure 7. MDM4 functions in the cytoplasmic compartment. (**a**) WB analysis of indicated proteins in nuclear (NUC), cytoplasmic (CYTO) and whole-cell extracts (WCEs) of si*MDM4*-MCF10A or si*CTL*-MCF10A cells treated with 2 μM Adr for 5 h. Ratio of densitometric values of HIPK2 to Tubulin (in the cytoplasm) or to SP1 (in the nucleus) levels is shown at the bottom of the blot. HIPK2/TUB ratio from control lane was arbitrarily set to 1. (**b**) WB of indicated proteins in NUC and CYTO extracts of si*MDM4*-MCF10A or si*CTL*-MCF10A in the presence or absence of importinα3 interference (si*KPNA4*) and treated as in a. Ratio of densitometric values of HIPK2 to Tubulin levels is shown at the bottom of the blot. HIPK2/TUB ratio from control lane was arbitrarily set to 1.

for cells to evade cell death. In fact, MDM4 localization is predominantly nuclear in tumour cell lines and many studies have increasingly reported nuclear localization of MDM4 in human tumour samples[60,61] suggesting this as an additional mechanism for deregulation of MDM4 activity in human cancer.

MATERIALS AND METHODS

Cell cultures and treatments

H1299, U2OS, HCT116 cells were maintained in DMEM/10% FBS (Life Technologies Italia, Monza, Italy), $Mdm4^{-/-}p53^{-/-}$ MEFs in DMEM high glucose/10% FBS (Cambrex, East Rutherford, NJ, USA), MCF10A and HMEC cells in MEGM (Lonza, Basilea, Switzerland). Plasmid pcDNA3.1MDM4106-360 was obtained by PCR amplification of fragments of the human Mdm4 cDNA with a specific pair of primers (available on request). MDM4, HIPK2 and control (CTL) siRNA were stealth RNAi (Life Technologies Italia).

Mouse maintenance and treatment

Control and transgenic mice were maintained and treated in accordance with the Guidelines on the protection of animals used for scientific purposes (European Directive 63/2010/EU and Italian Law DL116/1992 and DL 26/2014). For irradiation, female mice were exposed to whole body irradiation with a ^{137}Cs γ-irradiator (Protocol No. 12/2011 4714/2011). C57Bl/6 mice were obtained from CNR EMMA-INFRAFRONTIER-IMPC, 'A. Buzzati-Traverso' International Campus, Monterotondo Scalo.

ChIP

HCT116 DNA preparation was performed as previously described.[62] Immunoprecipitation was carried out with anti-p53 sheep polyclonal antibody, and relative normal sheep serum used as a negative control (Ab-7 and NSS, respectively; Calbiochem-Merck-Millipore, Darmstadt, Germany). Primer pairs, H1, H2 and H3 (available on request) that amplify human LGALS3 promoter were used for RT–qPCR by SYBR-Green PCR Master Mix (Life Technologies Italia).

Immunoprecipitation and WB analysis

Ip and WB were performed as previously described.[9] Primary antibodies used were: anti-MDM4 BL1258 (Bethyl Laboratory, Montgomery, TX, USA), anti-MDM4 C82, anti-α-tubulin DM1A, anti-actin C-40 (Sigma-Aldrich, St Louis, MO, USA), anti-p53 FL393 (Santa Cruz Biotechnology, Dallas, TX, USA), anti-p53Ser46^{P}, anti-p53 1C12 (Cell Signaling, Merck-Millipore, Darmstadt, Germany), p53Ser46^{P} (Becton Dickinson, Franklin Lakes, NJ, USA), anti-HIPK2 (by L. Schmitz), anti-MDM2 2A10 (by ME. Perry) and Ab1 (Calbiochem-Merck-Millipore), anti-ITGB4 (provided by R. Falcioni), anti-LGALS3 (Mabtech, Nacka Strand, Swedish), anti-SOD2 110 (Assay Designs, Enzo Life Sciences, New York, NY, USA), anti-GFP (Roche, Basel, Switzerland). Blots has been developed by chemiluminescence imaging system, Alliance 2.7 (UVITEC, Cambridge, UK) and quantified by the software Alliance V_1607.

Cell apoptosis and cell cycle analyses

Cell cycle profiles were evaluated as previously reported.[9] Annexin V and PI staining were performed by AnnexinV-FITC and/or PI (Clontech, Mountain

View, CA, USA). FACScan flowcytometer (Becton Dickinson) was used and data analysed by CellQuest Software (Becton Dickinson). TUNEL assays was performed with In Situ Cell Death Detection Kit (Roche).

Adenoviruses and lentivirus infection

Recombinant adenovirus were previously described.[5] The FH1t-UTG Mdm4 3′ UTR-GFP lentiviral construct was obtained by Marine's Lab by cloning shRNA sequence for MDM4-3′UTR (ACAGTCCTTCAGCTATTTCATTTCAAG AGAATGAAATAGCTGAAGGACTGTTTTTT) into the FH1tUTG vector, which constitutively expresses GFP.[63] MCF10A cells were infected with FH1t-UTG Mdm4 3′ UTR-GFP lentivirus to generate MCF10A-tet-shMDM4 inducible cell line.

RNA preparation and RT-PCR

RT–qPCR was performed with following primers: upperHIPK2 5′-AGGAA GAGTAAGCAGCACCAG-3′; lower HIPK2 5′-TGCTGATGGTGATGACACTGA-3′; upper hTBP 5′-GAACATCATGGATCAGAACAACA-3′; lower hTBP 5′-ATAGGG ATTCCGGGAGTCAT-3′; upper ITGB4: 5′-CACCGCGTGCTAAGCACAT-3′; lower ITGB4: 5′-TGTGGTCGAGTGTGAGTGTTCTG-3′; upper SOD2: 5′-GGCCTACGT GAACAACCTGAA-3′; lowerSOD2: 5′-CTGTAACATCTCCCTTGGCCA-3′; upper-LGALS3 5′-TCCACTTTAACCCACGCTTC-3′; lowerLGALS3 5′-TCTTCCCTTCC CCAGTTATT-3′; upperp53 5′-GTCTGGGCTTCTTGCATTCT-3′; lowerp53 5′-AATCAACCCACAGCTGCAC-3′. Amplification reactions were in triplicate and average of threshold cycles was used to interpolate standard curves and calculate transcript amount using the software SDS version 2.3 (Applied-Biosystems, Life Technologies Italia).

Immunofluorescence

Mdm4$^{-/-}$*p53*$^{-/-}$ MEFs cells were fixed with 2% formaldehyde, permeabilized with 0.25% TritonX100 and blocked with 5% BSA. Cells were stained with αMDM4 4B5 (OriGene, Rockville, MD, USA). Cyanine (Cy3)-conjugated secondary antibody was used.

Immunohistochemistry

Tissue breast samples were fixed in 4% formalin and within 24 h embedded in paraffin and 2-μm thick sections were used. After antigen retrieval with Heat-Induced Epitope Retrieval pH 6, slides were incubated with Mouse to Mouse Block for 40 min and stained with primary antibodies (αp53, CM5, 1:400, Novocastra; αGal-3, 1:200, Mabtech-AB, αHIPK2 from Soddu's lab[64]) for 25 min at RT. Detection was performed with EnVision FLEX/HRP (Dako Italia, Cernusco sul Naviglio, Italia) and developed with 3-3′diaminobenzidine system and counterstained with Harris' Haematoxylin using Mouse-To-mouse HRP (DAB) Staining System (ScyTek Laboratories, Logan, UT, USA). Microscope Leica BM5000 (Leica Microsystems, Nussloch, Germany) was used for optical evaluation.

Proteomic and bioinformatic analyses

The Shotgun proteomic analysis was performed on proteins extracted from cytoplasmic cell lysate of MCF10 cells. Continuum LC–MS data from three replicates experiments for each samples were processed for qualitative and quantitative analysis using ProteinLynx Global Server v. 2.3 (PLGS, Waters Co., Manchester, UK). Qualitative identification of proteins was obtained with the embedded ion accounting algorithm of the software PLGS, searching in the human database UniProt KB/Swiss-Prot Protein Knowledgebase release 2011_06 of 31-May-11 to which data from Saccharomyces cerevisiae Enolase was appended (UniProtKB/Swiss-Prot AC: P00924). Proteomic analysis was performed according to Pieroni *et al.*[65] Data were analyzed through the use of QIAGEN's Ingenuity Pathway Analysis, IPA (QIAGEN, Redwood City, CA, USA). Further details are available upon request.

CONFLICT OF INTEREST

The authors declare no conflict of interest.

ACKNOWLEDGEMENTS

The work was supported by research grants from Associazione Italiana Ricerca sul Cancro (AIRC; IG-8825, IG-12767) and from the Italian Ministry of Economy and Finance to the CNR for the Project 'FaReBio di Qualita' to FM; by FIRB RBAP1153LS_007 to AP; by FIRB: RBAP11WCRZ_003 to AU. LP and LF were supported by Susan Komen Italia Fellowship. We are grateful to Dr JC Marine for *Mdm4*$^{-/-}$*p53*$^{-/-}$ MEFs and lentiviral vectors, Dr L Schmith for polyclonal αHIPK2 antibody and Dr Cinzia Rinaldo for pSuper.retro-ip53 plasmid.

REFERENCES

1 Kawai H, Lopez-Pajares V, Kim MM, Wiederschain D, Yuan ZM. RING domain-mediated interaction is a requirement for MDM2's E3 ligase activity. *Cancer Res* 2007; **67**: 6026–6030.
2 Wang X, Wang J, Jiang X. MdmX protein is essential for Mdm2 protein-mediated p53 polyubiquitination. *J Biol Chem* 2011; **286**: 23725–23734.
3 Biderman L, Manley JL, Prives C. Mdm2 and MdmX as regulators of gene expression. *Genes Cancer* 2012; **3**: 264–273.
4 Migliorini D, Danovi D, Colombo E, Carbone R, Pelicci PG, Marine JC. Hdmx recruitment into the nucleus by Hdm2 is essential for its ability to regulate p53 stability and transactivation. *J Biol Chem* 2002; **277**: 7318–7323.
5 Mancini F, Gentiletti F, D'Angelo M, Giglio S, Nanni S, D'Angelo C *et al.* MDM4 (MDMX) overexpression enhances stabilization of stress-induced p53 and promotes apoptosis. *J Biol Chem* 2004; **279**: 8169–8180.
6 Barboza JA, Iwakuma T, Terzian T, El-Naggar AK, Lozano G. Mdm2 and Mdm4 loss regulates distinct p53 activities. *Mol Cancer Res* 2008; **6**: 947–954.
7 Lenos K, de Lange J, Teunisse AF, Lodder K, Verlaan-de Vries M, Wiercinska E *et al.* Oncogenic functions of hMDMX in in vitro transformation of primary human fibroblasts and embryonic retinoblasts. *Mol Cancer* 2011; **10**: 111.
8 Tsvetkov P, Reuven N, Prives C, Shaul Y. Susceptibility of p53 unstructured N terminus to 20S proteasomal degradation programs the stress response. *J Biol Chem* 2009; **284**: 26234–26242.
9 Mancini F, Di Conza G, Pellegrino M, Rinaldo C, Prodosmo A, Giglio S *et al.* MDM4 (MDMX) localizes at the mitochondria and facilitates the p53-mediated intrinsic-apoptotic pathway. *EMBO J* 2009; **28**: 1926–1939.
10 Zhu Y, Regunath K, Jacq X, Prives C. Cisplatin causes cell death via TAB1 regulation of p53/MDM2/MDMX circuitry. *Genes Dev* 2013; **27**: 1739–1751.
11 Wang CL, Wang JY, Liu ZY, Ma XM, Wang XW, Jin H *et al.* Ubiquitin-specific protease 2a stabilizes MDM4 and facilitates the p53-mediated intrinsic apoptotic pathway in glioblastoma. *Carcinogenesis* 2014; **35**: 1500–1509.
12 Migliorini D, Lazzerini Denchi E, Danovi D, Jochemsen A, Capillo M, Gobbi A *et al.* Mdm4 (Mdmx) regulates p53-induced growth arrest and neuronal cell death during early embryonic mouse development. *Mol Cell Biol* 2002; **22**: 5527–5538.
13 Oda K, Arakawa H, Tanaka T, Matsuda K, Tanikawa C, Mori T *et al.* p53AIP1, a potential mediator of p53-dependent apoptosis, and its regulation by Ser-46-phosphorylated p53. *Cell* 2000; **102**: 849–862.
14 Feng L, Hollstein M, Xu Y. Ser46 phosphorylation regulates p53-dependent apoptosis and replicative senescence. *Cell Cycle* 2006; **5**: 2812–2819.
15 Mayo LD, Seo YR, Jackson MW, Smith ML, Rivera Guzman J, Korgaonkar CK *et al.* Phosphorylation of human p53 at serine 46 determines promoter selection and whether apoptosis is attenuated or amplified. *J Biol Chem* 2005; **280**: 25953–25959.
16 Hofmann TG, Moller A, Sirma H, Zentgraf H, Taya Y, Dröge W *et al.* Regulation of p53 activity by its interaction with homeodomain-interacting protein kinase-2. *Nat Cell Biol* 2002; **4**: 1–10.
17 Cecchinelli B, Lavra L, Rinaldo C, Iacovelli S, Gurtner A, Gasbarri A *et al.* Repression of the antiapoptotic molecule galectin-3 by homeodomain-interacting protein kinase 2-activated p53 is required for p53-induced apoptosis. *Mol Cell Biol* 2006; **26**: 4746–4757.
18 Bon G, Di Carlo SE, Folgiero V, Avetrani P, Lazzari C, D'Orazi G *et al.* Negative regulation of beta4 integrin transcription by homeodomain-interacting protein kinase 2 and p53 impairs tumor progression. *Cancer Res* 2009; **69**: 5978–5986.
19 Sorrentino G, Mioni M, Giorgi C, Ruggeri N, Pinton P, Moll U *et al.* The prolyl-isomerase Pin1 activates the mitochondrial death program of p53. *Cell Death Differ* 2013; **20**: 198–208.
20 Pant V, Xiong S, Iwakuma T, Quintas-Cardama A, Lozano G. Heterodimerization of Mdm2 and Mdm4 is critical for regulating p53 activity during embryogenesis but dispensable for p53 and Mdm2 stability. *Proc Natl Acad Sci USA* 2011; **108**: 11995–12000.
21 Huang L, Yan Z, Liao X, Li Y, Yang J, Wang ZG *et al.* The p53 inhibitors MDM2/MDMX complex is required for control of p53 activity in vivo. *Proc Natl Acad Sci USA* 2011; **108**: 12001–12006.
22 Calzado MA, Renner F, Roscic A, Schmitz ML. HIPK2: a versatile switchboard regulating the transcription machinery and cell death. *Cell Cycle* 2007; **6**: 139–143.
23 Puca R, Nardinocchi L, Givol D, D'Orazi G. Regulation of p53 activity by HIPK2: molecular mechanisms and therapeutical implications in human cancer cells. *Oncogene* 2010; **29**: 4378–4387.

24 Rinaldo C, Prodosmo A, Mancini F, Iacovelli S, Sacchi A, Moretti F *et al.* MDM2-regulated degradation of HIPK2 prevents p53Ser46 phosphorylation and DNA damage-induced apoptosis. *Mol Cell* 2007; **25**: 739–750.
25 Lowe SW, Ruley HE, Jacks T, Housman DE. p53-dependent apoptosis modulates the cytotoxicity of anticancer agents. *Cell* 1993; **74**: 957–967.
26 Enge M, Bao W, Hedstrom E, Jackson SP, Moumen A, Selivanova G. MDM2-dependent downregulation of p21 and hnRNP K provides a switch between apoptosis and growth arrest induced by pharmacologically activated p53. *Cancer Cell* 2009; **15**: 171–183.
27 Latonen L, Taya Y, Laiho M. UV-radiation induces dose-dependent regulation of p53 response and modulates p53-HDM2 interaction in human fibroblasts. *Oncogene* 2001; **20**: 6784–6793.
28 Parant J, Chavez-Reyes A, Little NA, Yan W, Reinke V, Jochemsen AG *et al.* Rescue of embryonic lethality in Mdm4-null mice by loss of Trp53 suggests a non-overlapping pathway with MDM2 to regulate p53. *Nat Genet* 2001; **29**: 92–95.
29 Di Conza G, Mancini F, Buttarelli M, Pontecorvi A, Trimarchi F, Moretti F. MDM4 enhances p53 stability by promoting an active conformation of the protein upon DNA damage. *Cell Cycle* 2012; **11**: 749–760.
30 Stad R, Little NA, Xirodimas DP, Frenk R, van der Eb AJ, Lane DP *et al.* Mdmx stabilizes p53 and Mdm2 via two distinct mechanisms. *EMBO Rep* 2001; **2**: 1029–1034.
31 Rinaldo C, Moncada A, Gradi A, Ciuffini L, D'Eliseo D, Siepi F *et al.* HIPK2 controls cytokinesis and prevents tetraploidization by phosphorylating histone H2B at the midbody. *Mol Cell* 2012; **47**: 87–98.
32 Chen L, Gilkes DM, Pan Y, Lane WS, Chen J. ATM and Chk2-dependent phosphorylation of MDMX contribute to p53 activation after DNA damage. *EMBO J* 2005; **24**: 3411–3422.
33 Giglio S, Mancini F, Pellegrino M, Di Conza G, Puxeddu E, Sacchi A *et al.* Regulation of MDM4 (MDMX) function by p76(MDM2): a new facet in the control of p53 activity. *Oncogene* 2010; **29**: 5935–5945.
34 Silva JC, Denny R, Dorschel CA, Gorenstein M, Kass IJ, Li GZ *et al.* Quantitative proteomic analysis by accurate mass retention time pairs. *Anal Chem* 2005; **77**: 2187–2200.
35 Mirza A, Wu Q, Wang L, McClanahan T, Bishop WR, Gheyas F *et al.* Global transcriptional program of p53 target genes during the process of apoptosis and cell cycle progression. *Oncogene* 2003; **22**: 3645–3654.
36 Kho PS, Wang Z, Zhuang L, Li Y, Chew JL, Ng HH *et al.* p53-regulated transcriptional program associated with genotoxic stress-induced apoptosis. *J Biol Chem* 2004; **279**: 21183–21192.
37 Kracikova M, Akiri G, George A, Sachidanandam R, Aaronson SA. A threshold mechanism mediates p53 cell fate decision between growth arrest and apoptosis. *Cell Death Differ* 2013; **20**: 576–588.
38 Drane P, Bravard A, Bouvard V, May E. Reciprocal down-regulation of p53 and SOD2 gene expression-implication in p53 mediated apoptosis. *Oncogene* 2001; **20**: 430–439.
39 D'Orazi G, Cecchinelli B, Bruno T, Manni I, Higashimoto Y, Saito S *et al.* Homeodomain-interacting protein kinase-2 phosphorylates p53 at Ser 46 and mediates apoptosis. *Nat Cell Biol* 2002; **4**: 11–19.
40 Xiong S, Pant V, Suh YA, Van Pelt CS, Wang Y, Valentin-Vega YA *et al.* Spontaneous tumorigenesis in mice overexpressing the p53-negative regulator Mdm4. *Cancer Res* 2010; **70**: 7148–7154.
41 Marchenko ND, Hanel W, Li D, Becker K, Reich N, Moll UM. Stress-mediated nuclear stabilization of p53 is regulated by ubiquitination and importin-alpha3 binding. *Cell Death Differ* 2010; **17**: 255–267.
42 Kim YH, Choi CY, Lee SJ, Conti MA, Kim Y. Homeodomain-interacting protein kinases, a novel family of co-repressors for homeodomain transcription factors. *J Biol Chem* 1998; **273**: 25875–25879.
43 Moller A, Sirma H, Hofmann TG, Rueffer S, Klimczak E, Dröge W *et al.* PML is required for homeodomain-interacting protein kinase 2 (HIPK2)-mediated p53 phosphorylation and cell cycle arrest but is dispensable for the formation of HIPK domains. *Cancer Res* 2003; **63**: 4310–4314.
44 Di Stefano V, Rinaldo C, Sacchi A, Soddu S, D'Orazi G. Homeodomain-interacting protein kinase-2 activity and p53 phosphorylation are critical events for cisplatin-mediated apoptosis. *Exp Cell Res* 2004; **293**: 311–320.
45 Nardinocchi L, Puca R, D'Orazi G. HIF-1alpha antagonizes p53-mediated apoptosis by triggering HIPK2 degradation. *Aging (Albany NY)* 2011; **3**: 33–43.
46 Brooks CL, Gu W. The impact of acetylation and deacetylation on the p53 pathway. *Protein Cell* 2011; **2**: 456–462.
47 Mancini F, Moretti F. Mitochondrial MDM4 (MDMX) An unpredicted role in the p53-mediated intrinsic apoptotic pathway. *Cell Cycle* 2009; **8**: 3854–3859.
48 Mancini F, Di Conza G, Monti O, Macchiarulo A, Pellicciari R, Pontecorvi A *et al.* Puzzling over MDM4-p53 network. *Int J Biochem Cell Biol* 2010; **42**: 1080–1083.
49 Hanahan D, Weinberg RA. Hallmarks of cancer: the next generation. *Cell* 2011; **144**: 646–674.
50 Shaw LM, Rabinovitz I, Wang HH, Toker A, Mercurio AM. Activation of phosphoinositide 3-OH kinase by the alpha6beta4 integrin promotes carcinoma invasion. *Cell* 1997; **91**: 949–960.
51 Nakahara S, Oka N, Raz A. On the role of galectin-3 in cancer apoptosis. *Apoptosis* 2005; **10**: 267–275.
52 Werner ME, Chen F, Moyano JV, Yehiely F, Jones JC, Cryns VL. Caspase proteolysis of the integrin beta4 subunit disrupts hemidesmosome assembly, promotes apoptosis, and inhibits cell migration. *J Biol Chem* 2007; **282**: 5560–5569.
53 Lecona E, Barrasa JI, Olmo N, Llorente B, Turnay J, Lizarbe MA. Upregulation of annexin A1 expression by butyrate in human colon adenocarcinoma cells: role of p53, NF-Y, and p38 mitogen-activated protein kinase. *Mol Cell Biol* 2008; **28**: 4665–4674.
54 Chiu CG, Strugnell SS, Griffith OL, Jones SJ, Gown AM, Walker B *et al.* Diagnostic utility of galectin-3 in thyroid cancer. *Am J Pathol* 2010; **176**: 2067–2081.
55 Lipscomb EA, Simpson KJ, Lyle SR, Ring JE, Dugan AS, Mercurio AM. The alpha6beta4 integrin maintains the survival of human breast carcinoma cells in vivo. *Cancer Res* 2005; **65**: 10970–10976.
56 Li Q, Lin S, Wang X, Lian G, Lu Z, Guo H *et al.* Axin determines cell fate by controlling the p53 activation threshold after DNA damage. *Nat Cell Biol* 2009; **11**: 1128–1134.
57 Sykes SM, Mellert HS, Holbert MA, Li K, Marmorstein R, Lane WS *et al.* Acetylation of the p53 DNA-binding domain regulates apoptosis induction. *Mol Cell* 2006; **24**: 841–851.
58 Tang Y, Luo J, Zhang W, Gu W. Tip60-dependent acetylation of p53 modulates the decision between cell-cycle arrest and apoptosis. *Mol Cell* 2006; **24**: 827–839.
59 Kreuzaler P, Watson CJ. Killing a cancer: what are the alternatives? *Nat Rev Cancer* 2012; **12**: 411–424.
60 Leventaki V, Rodic V, Tripp SR, Bayerl MG, Perkins SL, Barnette P *et al.* TP53 pathway analysis in paediatric Burkitt lymphoma reveals increased MDM4 expression as the only TP53 pathway abnormality detected in a subset of cases. *Br J Haematol* 2012; **158**: 763–771.
61 Gembarska A, Luciani F, Fedele C, Russell EA, Dewaele M, Villar S *et al.* MDM4 is a key therapeutic target in cutaneous melanoma. *Nat Med* 2012; **18**: 1239–1247.
62 Boyd KE, Wells J, Gutman J, Bartley SM, Farnham PJ. c-Myc target gene specificity is determined by a post-DNAbinding mechanism. *Proc Natl Acad Sci USA* 1998; **95**: 13887–13892.
63 Herold MJ, van den Brandt J, Seibler J, Reichardt HM. Inducible and reversible gene silencing by stable integration of an shRNA-encoding lentivirus in transgenic rats. *Proc Natl Acad Sci USA* 2008; **105**: 18507–18512.
64 Iacovelli S, Ciuffini L, Lazzari C, Bracaglia G, Rinaldo C, Prodosmo A *et al.* HIPK2 is involved in cell proliferation and its suppression promotes growth arrest independently of DNA damage. *Cell Prolif* 2009; **42**: 373–384.
65 Pieroni L, Finamore F, Ronci M, Mattoscio D, Marzano V, Mortera SL *et al.* Proteomics investigation of human platelets in healthy donors and cystic fibrosis patients by shotgun nUPLC-MSE and 2DE: a comparative study. *Mol Biosyst* 2011; **7**: 630–639.

Supplementary Information accompanies this paper on the Oncogene website (http://www.nature.com/onc)